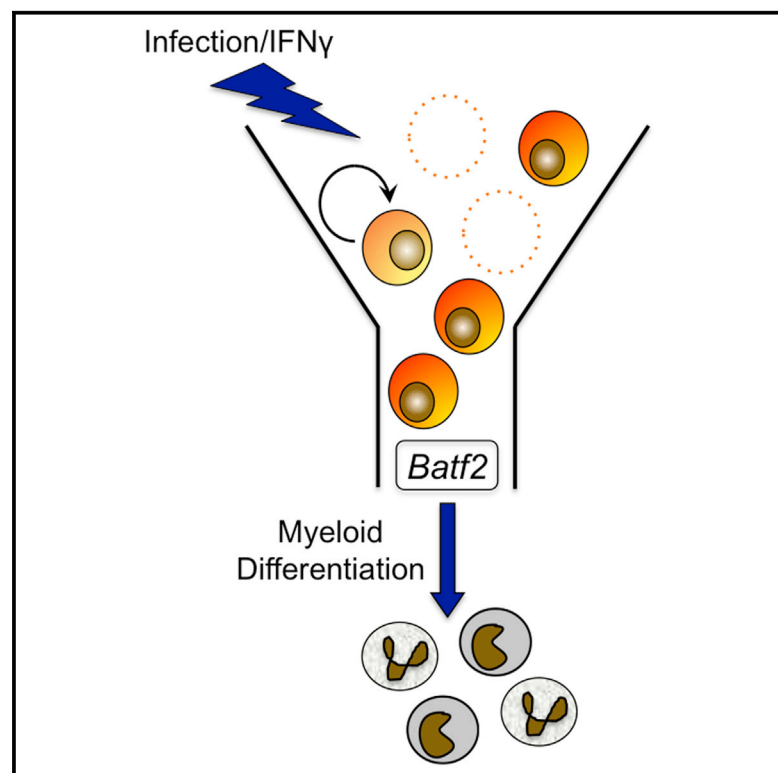


## Chronic Infection Depletes Hematopoietic Stem Cells through Stress-Induced Terminal Differentiation

### Graphical Abstract



### Authors

Katie A. Matatall, Mira Jeong, Siyi Chen, ..., Qianxing Mo, Marek Kimmel, Katherine Y. King

### Correspondence

kyk@bcm.edu

### In Brief

Matatall et al. show that chronic infection causes pancytopenia and hematopoietic stem cell (HSC) depletion in mice. HSCs are lost through impaired self-renewal and increased terminal differentiation, which can be triggered by induction of the interferon gamma-responsive transcription factor BATF2. This study elucidates mechanisms underlying bone marrow failure during chronic infections.

### Highlights

- Chronic *M. avium* infection causes pancytopenia in mice
- Chronic *M. avium* infection depletes the hematopoietic stem cell (HSC) pool
- Terminal differentiation is the major route of HSC loss during infection
- The transcription factor BATF2 promotes IFN- $\gamma$ -dependent HSPC differentiation

### Accession Numbers

GSE89364



# Chronic Infection Depletes Hematopoietic Stem Cells through Stress-Induced Terminal Differentiation

Katie A. Matatall,<sup>1,2,5</sup> Mira Jeong,<sup>2,5</sup> Siyi Chen,<sup>7</sup> Deqiang Sun,<sup>6</sup> Fengju Chen,<sup>4</sup> Qianxing Mo,<sup>4</sup> Marek Kimmel,<sup>7,8</sup> and Katherine Y. King<sup>1,2,3,4,5,9,\*</sup>

<sup>1</sup>Section of Pediatric Infectious Diseases

<sup>2</sup>Center for Cell and Gene Therapy

<sup>3</sup>BCM Inflammation Center

<sup>4</sup>Dan L. Duncan Cancer Center

<sup>5</sup>Stem Cells and Regenerative Medicine Center

Baylor College of Medicine, Houston, TX 77030, USA

<sup>6</sup>Institute of Biosciences & Technology, College of Medicine Texas A&M University Health Science Center, Houston, TX 77030, USA

<sup>7</sup>Department of Statistics, Rice University, Houston, TX 77030, USA

<sup>8</sup>Systems Engineering Group, Silesian University of Technology, Akademicka 16, 44-100 Gliwice, Poland

<sup>9</sup>Lead Contact

\*Correspondence: [kyk@bcm.edu](mailto:kyk@bcm.edu)

<http://dx.doi.org/10.1016/j.celrep.2016.11.031>

## SUMMARY

Chronic infections affect a third of the world's population and can cause bone marrow suppression, a severe condition that increases mortality from infection. To uncover the basis for infection-associated bone marrow suppression, we conducted repeated infection of WT mice with *Mycobacterium avium*. After 4–6 months, mice became pancytopenic. Their hematopoietic stem and progenitor cells (HSPCs) were severely depleted and displayed interferon gamma (IFN- $\gamma$ ) signaling-dependent defects in self-renewal. There was no evidence of increased HSPC mobilization or apoptosis. However, consistent with known effects of IFN- $\gamma$ , transcriptome analysis pointed toward increased myeloid differentiation of HSPCs and revealed the transcription factor *Batf2* as a potential mediator of IFN- $\gamma$ -induced HSPC differentiation. Gain- and loss-of-function studies uncovered a role for *Batf2* in myeloid differentiation in both murine and human systems. We thus demonstrate that chronic infection can deplete HSPCs and identify *BATF2* as a mediator of infection-induced HSPC terminal differentiation.

## INTRODUCTION

Chronic infections including tuberculosis (2 billion infected worldwide; CDC), hepatitis C virus (180 million; WHO), and HIV (34 million; NIH) are estimated to affect over a third of the world's population. These diseases are associated with significant health implications including bone marrow suppression and an increased risk for cancer (Ramos-Casals et al., 2003; Scadden et al., 1989). Pancytopenia, a suppression of blood counts across multiple lineages, can affect as many as 12% of people

with disseminated or miliary tuberculosis and increases risk of death from the infection (Achi et al., 2013). Collectively, these observations suggest that chronic infections may significantly affect the function of hematopoietic stem cells (HSCs), the progenitor cells of all blood cells. Thus, understanding the long-term effects of inflammation on HSC number and function is a matter of key clinical importance.

Production of blood cells by the bone marrow is a highly dynamic process. An estimated  $10^{11}$ – $10^{12}$  blood cells are produced by hematopoietic progenitors in the bone marrow on a daily basis, and this number increases during infection (Takizawa et al., 2012). Primitive hematopoietic stem and progenitor cells (HSPCs) are the precursors of all cells of the peripheral blood (PB) and are responsible for maintaining healthy blood production. HSPCs include not only long-term HSCs, which have self-renewal capacity, but also multipotent progenitors (MPPs), which do not. Recent work suggests that HSPCs can generate restricted subsets of terminally differentiated progeny, bypassing the stepwise progression through common myeloid progenitor (CMP) and common lymphoid progenitor (CLP) stages (Notta et al., 2016). Thus, directed differentiation of blood cells may be driven by signals that act at the earliest stages of the hematopoietic hierarchy.

In fact, HSCs are highly responsive to the inflammatory conditions that exist during a typical infection (Takizawa et al., 2012), and a variety of signals can affect HSC function during infection. HSCs express pathogen pattern recognition receptors such as Toll-like receptor 4. Bacterial products sensed by these receptors alter HSC quiescence and function (Balmer et al., 2014; Nagai et al., 2006). Inflammatory signals propagated by the immune system can also affect HSC function, and interferons (IFNs) are particularly powerful regulators of HSCs (King and Goodell, 2011). For example, IFN- $\alpha$  signaling can promote HSC division (Essers et al., 2009; Pietras et al., 2014). We previously showed that IFN- $\gamma$  stimulates cell division of HSCs in a murine model of *Mycobacterium avium* infection, leading to a defect in repopulation capacity (Baldridge

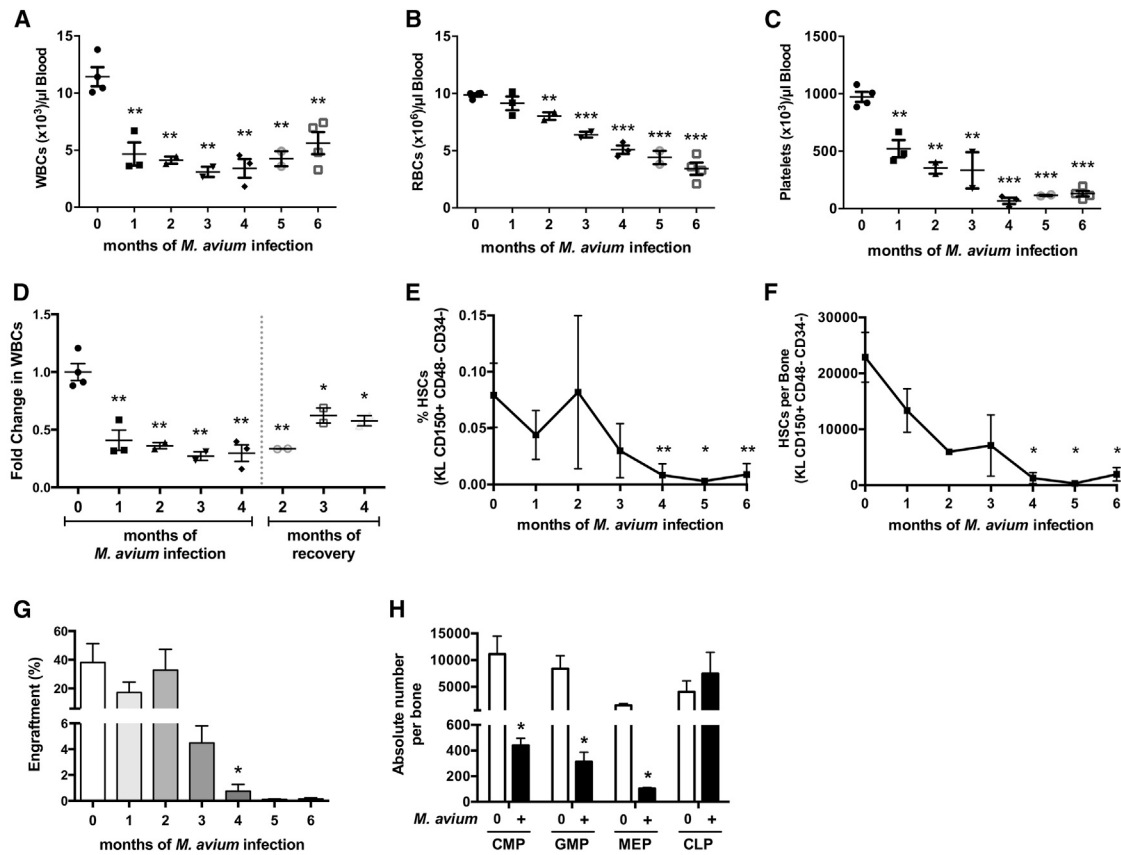


**Figure 1. Chronically Infected Mice Develop Pancytopenia and Severe HSC Loss**

(A–C) Mice were infected with *M. avium* every 4 weeks for 1–6 months. Bone marrow and PB were assessed 4 weeks after the final injection. (A) White blood cell (WBC), (B) red blood cell (RBC), and (C) platelet counts decline with chronic infection. (D) WBC counts do not recover following cessation of infections in 4-month-infected mice. (E and F) The number of HSCs (KL CD150<sup>+</sup> CD48<sup>-</sup> CD34<sup>-</sup>) after repeated *M. avium* infections. (E) Percentage of live WBM cells. (F) Absolute number per bone. (G) Total engraftment of PB, shown as percentage CD45.2 cells of total blood, 16 weeks after transplant.  $2 \times 10^5$  WBM cells from naive or infected animals (CD45.2) were mixed with  $2 \times 10^5$  rescue marrow (CD45.1) and transplanted into lethally irradiated mice. (H) Progenitor populations in the bone marrow of naive and 6-month infected mice, shown as absolute number of cells per bone. Data are presented as mean  $\pm$  SEM; \* $p < 0.05$ , \*\* $p < 0.01$ , \*\*\* $p < 0.001$ .

Data are representative of two (A–C, F, and G), three (E), or four (D) independent experiments;  $n = 3$ –5 per group. See also [Figure S1](#) and [Table S1](#).

et al., 2010). Furthermore, short-term IFN- $\gamma$ -mediated HSC division appears to accelerate differentiation during infection (Matatall et al., 2014); however, both the long-term impact and the mechanism of these processes remain unknown.

Here, we capitalize on our murine model of *M. avium* infection to evaluate the impact of chronic infection on the HSC pool. *M. avium* typically produces a chronic (~10 weeks) systemic IFN- $\gamma$ -mediated immune response in mice similar to what can be seen in patients with tuberculosis (Flórido et al., 2005). We show that chronic infection drives exhaustion of the HSC compartment, with depletion of both PB counts and HSC self-renewal capacity. We use this model to evaluate the mechanisms of HSC loss and identify a potential mediator of stress-induced myeloid specification. Our study thus provides direct evidence for how infections and persistent inflammation affect the HSC population and elicit diseases associated with HSC loss.

## RESULTS

### Chronically Infected Mice Develop Pancytopenia

To characterize the effects of chronic infection on bone marrow function, we conducted repeated monthly infections of mice with *M. avium*. PB of infected animals showed a progressive decline in all cell types, reaching statistical significance by 1–2 months of infection (Figures 1A–1C). Several mice appeared nearly moribund after 6 months. After 4 months, the hematopoietic effects of infection were irreversible (Figure 1D).

### Chronic Infection Depletes HSCs

We characterized hematopoietic progenitors in the bone marrow of chronically infected animals. The number of phenotypically defined long-term HSCs (lineage-negative, cKit-positive [LK] CD150<sup>+</sup> CD48<sup>-</sup> CD34<sup>-</sup>) declined during the course of infection; by 4 months of infection only 5.7% of the starting number of

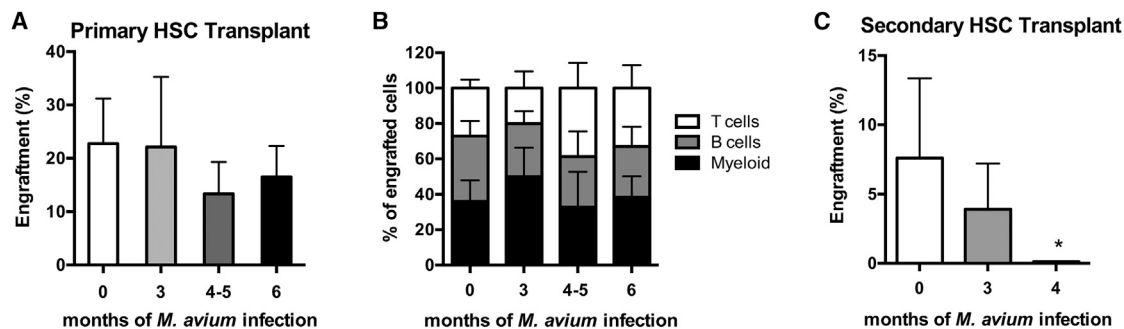


**Figure 2. HSCs from Chronically Infected Animals Have a Self-Renewal Defect**

(A and B) 300 sorted CD45.2 HSCs (SP<sup>LSK</sup> CD150<sup>+</sup>) from naive or *M. avium*-infected mice were transplanted with  $2 \times 10^5$  CD45.1 rescue marrow into lethally irradiated mice. Donor mice were infected with *M. avium* three, four, five, or six times (once every 4 weeks); the four- and five-dose mice were pooled before transplant. PB was assessed at 16 weeks post-transplant. (A) Total engraftment is shown as percentage of CD45.2 cells in total blood. (B) Lineage distribution of T cells, B cells, and myeloid cells is shown as percentage of total CD45.2 cells.

(C) Secondary transplant of 250 sorted CD45.2 HSCs (SP LSK CD150<sup>+</sup>) from previously transplanted animals. Donor HSCs were co-transplanted with  $2 \times 10^5$  CD45.1 rescue marrow into lethally irradiated mice. PB was assessed 16 weeks post-transplant, and engraftment is shown as percentage of CD45.2 cells in blood. Data are presented as mean  $\pm$  SEM; \* $p < 0.05$ . Except for secondary transplant done once with  $n = 5$  per group, data are representative of two independent experiments with  $n = 5$  per group.

HSCs remained (Figures 1E, 1F, S1B, and S1C). This decline in stem cell number outstripped the rate of weight loss (Figure S1A), suggesting that stem cell loss was not due to nutritional deficit. The stem cell marker Sca1 was intentionally excluded because it can be non-specifically activated during infection (Baldridge et al., 2011). In addition, we found that the number of myeloid-biased HSCs was more depressed than the lymphoid-biased HSCs (Figure S1D) (Matatall et al., 2014). This decrease was also manifest by a decline in the absolute number of myeloid cells derived from transplanted marrow (Figure S1E). There was a consistent rebound in the number of HSCs as a percentage of whole-bone marrow (WBM) at 2 months post-infection across four repetitions of the chronic infection experiment (Figure 1E), suggesting that the bone marrow can initially adapt to inflammatory responses but that such compensatory processes are eventually overwhelmed.

To assess the number of functionally defined HSCs in chronically infected animals, we transplanted  $2 \times 10^5$  WBM cells from infected animals with  $2 \times 10^5$  rescue marrow into lethally irradiated naive recipient animals. As shown in Figure 1G, WBM engraftment declined after chronic infection, mirroring the decline in phenotypically defined HSCs. To determine whether reduced engraftment was due to transmitted infection, we cultured WBM cells in methylcellulose, which does not support the growth of mycobacteria. WBM of chronically infected animals generated significantly fewer total cells after 9 days of incubation compared to control WBM, suggesting that loss of HSPCs was not due to direct infection of the cells (Figure S1F). Collectively, these data indicate that HSCs are depleted during chronic infection.

We quantified the presence of committed lymphoid and myeloid progenitors in the marrow during chronic infection. After 6 months of infection, the number of CLPs was steady, but the number of myeloid progenitors including CMPs, granulocyte-monocyte progenitors (GMPs), and megakaryocyte-erythrocyte progenitors (MEPs) was reduced (Figure 1G), indicating myeloid

progenitors are more easily exhausted during chronic *M. avium* infection than lymphoid progenitors.

### HSCs from Chronically Infected Animals Show a Self-Renewal Defect upon Secondary Transplant

To ascertain whether cell-autonomous defects occur in HSC function upon chronic infection, we sorted LT-HSCs (SP<sup>LSK</sup> CD150<sup>+</sup>) from naive or infected animals and transplanted 300 cells from transplanted cells was not affected by chronic infection (Figure 2B). These findings indicate that while the total number of LT-HSCs was decreased in chronically infected animals, their ability to reconstitute long-term hematopoiesis upon primary transplantation was not impaired.

To evaluate the self-renewal capacity of HSCs from infected animals, we conducted secondary transplant. Secondary engraftment of sorted HSCs from chronically infected mice was significantly diminished compared to HSCs from naive animals, and HSCs from animals that had been infected for the longest time were most severely affected (Figure 2C). Thus, secondary transplants revealed a self-renewal defect in HSCs from chronically infected mice, indicating that HSC exhaustion can occur following persistent infectious stimulation.

### Loss of HSCs Precedes Marrow Fibrosis

Most medical textbooks ascribe pancytopenia associated with chronic infections such as tuberculosis to marrow fibrosis (Fitzgerald and Haas, 2005). However, a causal relationship between myelofibrosis and bone marrow suppression during infection has not been firmly established (Viallard et al., 2002). Using trichrome staining, we found that patches of marrow fibrosis became evident after only 1 month of infection, but remained limited to small areas of the marrow through 6 months of infection

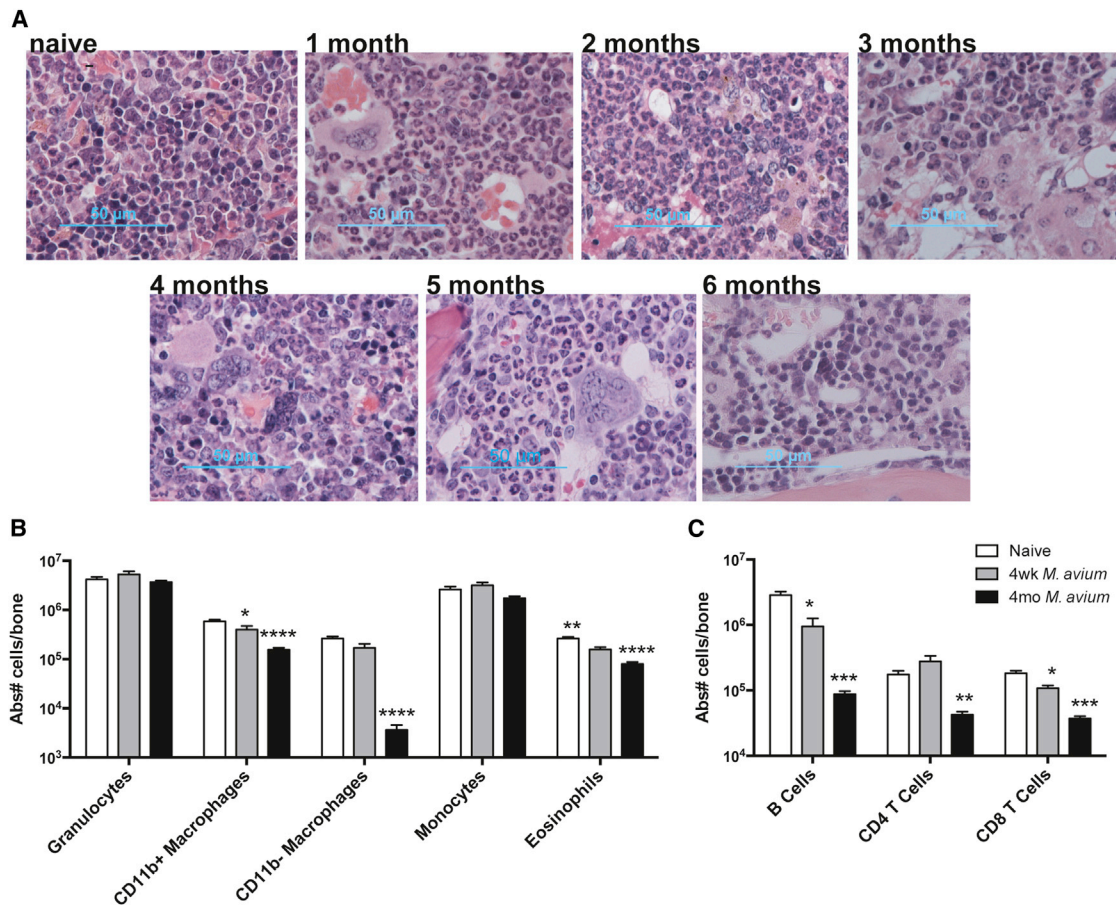


### Figure 3. Myeloid Cells Infiltrate Bone Marrow during Chronic Infection

(A) H&E-stained sections of bone marrow from naive and chronically infected animals.

(B and C) Flow cytometry of the WBM cells from naive, 1-month-, or 4-month-infected animals. Absolute number of cells per bone is shown. Data in (B) and (C) are presented as mean  $\pm$  SEM; \* $p < 0.05$ , \*\* $p < 0.01$ , \*\*\* $p < 0.001$ , \*\*\*\* $p < 0.0001$ .

Data are representative of two independent experiments with  $n = 4-7$  per group. See also Figures S2 and S3.

(Figure S2A). Overall, marrow of infected mice demonstrated progressively reduced cellularity (Figure S2B), but neither the loss in cellularity nor the degree of fibrosis was sufficient to account for the  $\sim 95\%$  loss in HSCs by 4 months of infection. H&E staining showed a relative increase of granulocytes and monocytes which was confirmed by flow cytometry (Figures 3A, 3B, S2C, and S3). Meanwhile, the absolute number of lymphoid cells in the bone marrow declined, with reductions in B and T cells (Figures 3C and S2D), and all classes of B cell precursors and immature T cells (Figures S2E and S2F). Altogether, these findings suggest that the rate of HSC loss outpaces the rate of marrow fibrosis and that inflammatory changes, including a relative increase in neutrophils and monocytes, can be seen during chronic infection.

### Impaired HSC Engraftment during *M. Avium* Infection Is IFN- $\gamma$ Dependent

IFN- $\gamma$  is a key immune mediator during mycobacterial infections and we previously showed that IFN- $\gamma$  alone can induce HSC division and differentiation (Baldrige et al., 2010). Here, we show

that IFN- $\gamma$  levels remained high in the serum of infected animals even after 6 months of infection (Figure 4A). We also demonstrate that IFN- $\gamma$  is highly expressed by both T and natural killer (NK) cells in the bone marrow of chronically infected animals (Figure S4A).

To investigate the role of IFN- $\gamma$  in impaired HSC function during infection, we infected wild-type (WT) or *Ifngr1*<sup>-/-</sup> mice with *M. avium* and then transplanted their marrow into WT recipients. We found that infection reduced the engraftment of HSCs from WT animals. The trend was reversed in infected *Ifngr1*<sup>-/-</sup> mice, with WBM from these mice engrafting at least as well as uninfected WT cells (Figure 4B). These findings suggest that IFN- $\gamma$ -dependent effects impair the capacity of WT marrow to engraft following infection. To confirm these findings, we created mosaic animals by transplanting either WT or *Ifngr1*<sup>-/-</sup> marrow into lethally irradiated WT recipients. Six weeks after transplant, we infected test animals with *M. avium*, whereas control animals were uninfected. Engraftment was significantly curtailed in recipients of infected WT marrow. In contrast, infection did not affect engraftment in *Ifngr1*<sup>-/-</sup> marrow recipients (Figure 4C).

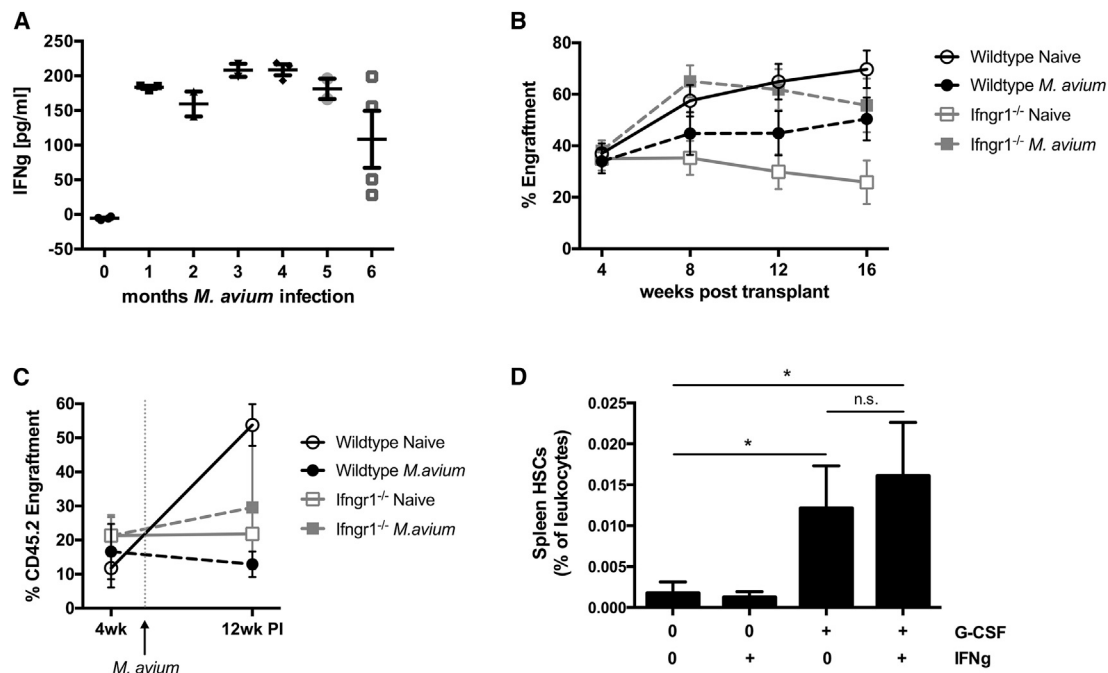


**Figure 4. Impaired HSC Engraftment after *M. avium* Infection Is IFN- $\gamma$  Dependent and Does Not Involve HSC Mobilization**

(A) Mice were infected with *M. avium* every 4 weeks for 1–6 months. IFN- $\gamma$  levels in serum of chronically infected mice determined by ELISA. One experiment with  $n = 2$ –5 per group.  
 (B) Engraftment of  $2 \times 10^5$  WBM cells from WT or Ifngr1<sup>-/-</sup> mice that were naive or infected for 1 month with *M. avium*. One experiment with  $n = 9$ –10 per group.  
 (C) Engraftment of WT or Ifngr1<sup>-/-</sup> mosaic transplants at 2 weeks pre- and 12 weeks post-infection. Mice were transplanted with either  $2 \times 10^5$  WT or  $3 \times 10^5$  Ifngr1<sup>-/-</sup> bone marrow with  $2 \times 10^5$  rescue marrow. Transplant recipients were infected with *M. avium* 6 weeks post-transplant. Data represent four independent experiments with  $n = 7$ –14 per group.  
 (D) The number of HSCs in the spleen was assessed in mice that had been treated with G-CSF and/or IFN- $\gamma$  and is shown as percentage of Lin<sup>+</sup>cKit<sup>+</sup>CD150<sup>+</sup>CD48<sup>-</sup> cells of total leukocytes. Data represent two independent experiments with  $n = 2$ –3 per group. Data are presented as mean  $\pm$  SEM; \* $p < 0.05$ , \*\* $p < 0.01$ , \*\*\* $p < 0.001$ , n.s., not significant. See also Figure S4.

Collectively, these findings suggest that functional deficits in HSCs during *M. avium* infection are attributable to IFN- $\gamma$  exposure via a cell-autonomous mechanism.

### Mathematical Modeling of HSC Loss during Chronic Infection

The decline in total HSC number during chronic infection implies an increase in the rate of HSC loss. To estimate the magnitude of HSC loss during infection, we created a mathematical model of hematopoiesis using differential equations based on steady state parameters: total number of HSCs, division rate, rate of self-renewal versus loss, and time (cf. Estimation of HSC Loss in the Experimental Procedures). We assumed that HSCs can be lost through death, differentiation, or displacement. Thus, we used an aggregate variable  $d$  to reflect the overall proportion of HSCs lost per division event, where  $d = 0.5$  indicates complete self-renewal and  $d = 1$  indicates complete loss (no progeny are HSCs). We applied our data from chronic infection to this model and concluded that the  $d$  must increase from  $d = 0.5$  at the steady state to a median value of 0.788 during chronic infection to account for the dramatic loss of HSCs observed (Figure S1G). In other words, whereas at steady state each HSC division produces one new HSC and one cell that is “lost” through differ-

entiation, displacement, or death, during infection the percentage of HSC loss goes up by 57%. As might be expected, we observed a very large inter-individual heterogeneity of the response, as reflected in the wide 95% confidence interval (0.729–0.954) for  $d$  (Figure S1H; Table S1).

### Infection Does Not Induce HSC Mobilization

We sought to understand the mechanism by which HSCs were lost during chronic infection. We previously reported that lineage-negative, Sca1-positive, cKit-positive (LSK) CD150<sup>+</sup>CD48<sup>-</sup> cells are increased in the spleens of *M. avium*-infected animals, suggesting that displacement from the bone marrow niche is a potential mechanism for HSC loss (Baldrige et al., 2010). However, a more recent report indicated that HSCs are not mobilized from bone marrow during chronic *E. chafeensis* infection (McCabe et al., 2015). We therefore performed mobilization studies using IFN- $\gamma$  and granulocyte colony-stimulating factor (G-CSF). While G-CSF increased the number of HSCs (LK CD150<sup>+</sup>CD48<sup>-</sup>CD34<sup>-</sup>Flk2<sup>+</sup>) in the spleen as expected, IFN- $\gamma$  treatment did not. Co-administration of IFN- $\gamma$  with G-CSF did not further boost the number of HSCs detectable in the spleen (Figure 4D). These results were confirmed upon transplantation of splenocytes from animals after G-CSF or IFN- $\gamma$

treatment (Figure S4B), suggesting that IFN- $\gamma$  does not induce HSC mobilization from the bone marrow.

### HSCs from Chronically Infected Animals Are Not Actively Apoptotic

We next considered cell death as a potential mechanism of HSC loss during chronic infection. We previously reported that HSCs are induced to divide during infection (Baldridge et al., 2010), and a recent report linked increased cell division with accumulation of DNA damage and attrition of HSCs by apoptosis (Walter et al., 2015). Furthermore, cell death can be triggered in HSCs upon secondary stress after IFN- $\alpha$  stimulation (Pietras et al., 2014). Therefore, we investigated whether persistent infection could impose increased replication stress on HSCs, leading to increased apoptosis. We confirmed that cell-cycle activity, determined by Ki67 staining, was high in HSCs even after months of infection (Figure 5A). Next, we measured reactive oxygen species (ROS) in the HSCs of infected animals. Compared to HSCs from naive animals, we saw no increase in ROS in LK CD150<sup>+</sup> CD48<sup>-</sup> HSCs (Figure 5B). However, we did note a slight increase in DNA damage in HSCs from chronically infected mice as measured by pKap1 staining and  $\gamma$ H2AX staining (Figures 5C and 5D), but these increases were minor compared to the degree of DNA damage measured in the positive controls.

To test for activation of apoptosis upon secondary stress, we incubated HSCs for 12 hr ex vivo and then measured caspase activation. Following this secondary stress, apoptosis was increased in HSCs from mice that had been infected for 1 or 3 months compared to controls (Figure 5E). To ascertain whether stress-induced apoptosis is related to IFN- $\gamma$  stimulation, we treated mice with recombinant IFN- $\gamma$  for 24 hr and then incubated HSCs from these mice for 12 hr ex vivo. The IFN- $\gamma$ -treated cells showed elevated caspase activation compared to HSCs from control mice (Figure 5F). We also compared the effect of *M. avium* infection on stress-induced apoptosis in WT versus *Ifrngr1*<sup>-/-</sup> mice. In contrast to WT, HSCs from infected *Ifrngr1*<sup>-/-</sup> mice did not show stress-induced apoptosis, again highlighting that this effect is IFN- $\gamma$  dependent (Figure S5A).

As a secondary measure of cell survival, we sorted HSCs singly into 96-well plates containing complete stem cell media. The number of colonies formed under these stressful ex vivo conditions was diminished for cells derived from mice that had been infected for 1 or 4 months or from animals treated with IFN- $\gamma$ , consistent with a lower threshold for apoptosis in these cells (Figure S5B). These findings indicate that chronic *M. avium* infection or transient IFN- $\gamma$  exposure can make HSCs more susceptible to apoptosis upon secondary stress.

As HSCs from infected or IFN- $\gamma$ -treated animals had an increased propensity for apoptosis following ex vivo secondary stress, we investigated whether the rate of apoptosis was increased during infection in vivo. We isolated HSCs from control or infected mice and immediately measured caspase activation (Figures 5G and S5C). Caspase activation was not noted in HSCs from naive or infected mice immediately after cell sorting and was far from the level that would have been required by mathematical models to account for the loss in HSC number. Thus, even though IFN- $\gamma$  stimulation can lower the threshold for apoptosis in HSCs, an increased rate of apoptosis was

not detectable among HSCs during in vivo infection. Therefore, we conclude that apoptosis alone cannot account for significant loss of HSCs observed during chronic infection in vivo (Figure S1G).

### Transcriptional Profiling of HSCs from Chronically Infected Animals Reveals Increased Differentiation

To further characterize potential mechanisms of HSC loss during chronic infection, we sorted HSCs from naive mice and mice infected for 1 month with *M. avium* and conducted whole-transcriptome analysis by RNA sequencing (Figure 6A; Table S2). HSCs from infected animals demonstrated increased expression of *Stat1*, *Cxcl9*, and the interferon responsive GTPase *Irgm1*, consistent with an ongoing TH1-type inflammatory response (Figure 6B) (King et al., 2011). Gene ontology analysis of the RNA sequencing (RNA-seq) data revealed a strong upregulation of genes associated with antigen processing and presentation and immune responses including major histocompatibility complex II genes, suggesting a shift toward gene expression signatures of myeloid cells such as macrophages and dendritic cells (Figure 6C). Genes related to apoptosis and cell death were strikingly absent, further supporting the lack of apoptosis noted in the studies described above. Upon gene set enrichment analysis (GSEA), the only major category significantly enriched was antigen processing and presentation (Figure 6D), pointing toward myeloid differentiation as the major transcriptional change occurring in HSCs during infection.

To understand the extent to which IFN- $\gamma$  promotes myeloid differentiation of HSPCs, we isolated CD34<sup>+</sup> cells from human Buffy coat samples and treated them with IFN- $\gamma$  in vitro. Within 3 days, the number of CD34<sup>+</sup>CD38<sup>-</sup> stem cells decreased by 7-fold compared to untreated control cells. Meanwhile, there was a dramatic increase in cells with the phenotype of differentiated myeloid cells, particularly CD15<sup>+</sup> myelomonocytic cells and CD66b<sup>+</sup> granulocytes, consistent with a prior report (Figures S6A and S6B) (Yang et al., 2005). These data show that IFN- $\gamma$  can induce a major shift toward differentiation in HSCs on a scale that would be sufficient to deplete the HSC population.

### Overexpression of *Batf2* Drives Myeloid Differentiation of HSPCs

We hypothesized that terminal differentiation may be the major mechanism of HSC loss during chronic infection. To identify molecular drivers of this process, we focused on the four transcription factors upregulated during infection. Aside from expected increases in expression of *Stat1*, *NfkbpaB*, and *Ciita*, *Batf2*, an IFN- $\gamma$ -responsive transcription factor, was significantly upregulated in HSCs during *M. avium* infection (Table S2; Figure 6B). This transcription factor caught our attention because it has been previously reported to participate in dendritic cell development during stress (Tussiwand et al., 2012). The *Batf2* family member *Batf* acts as a differentiation checkpoint that limits HSC self-renewal in response to DNA damage while promoting lymphoid differentiation (Santos et al., 2014; Wang et al., 2012). We assayed transcript levels from HSCs by qPCR and found that *Batf2* was upregulated 8-fold in HSCs during *M. avium* infection (Figure 7A). Furthermore, we found that *Batf2* was not induced when *M. avium* infection was conducted

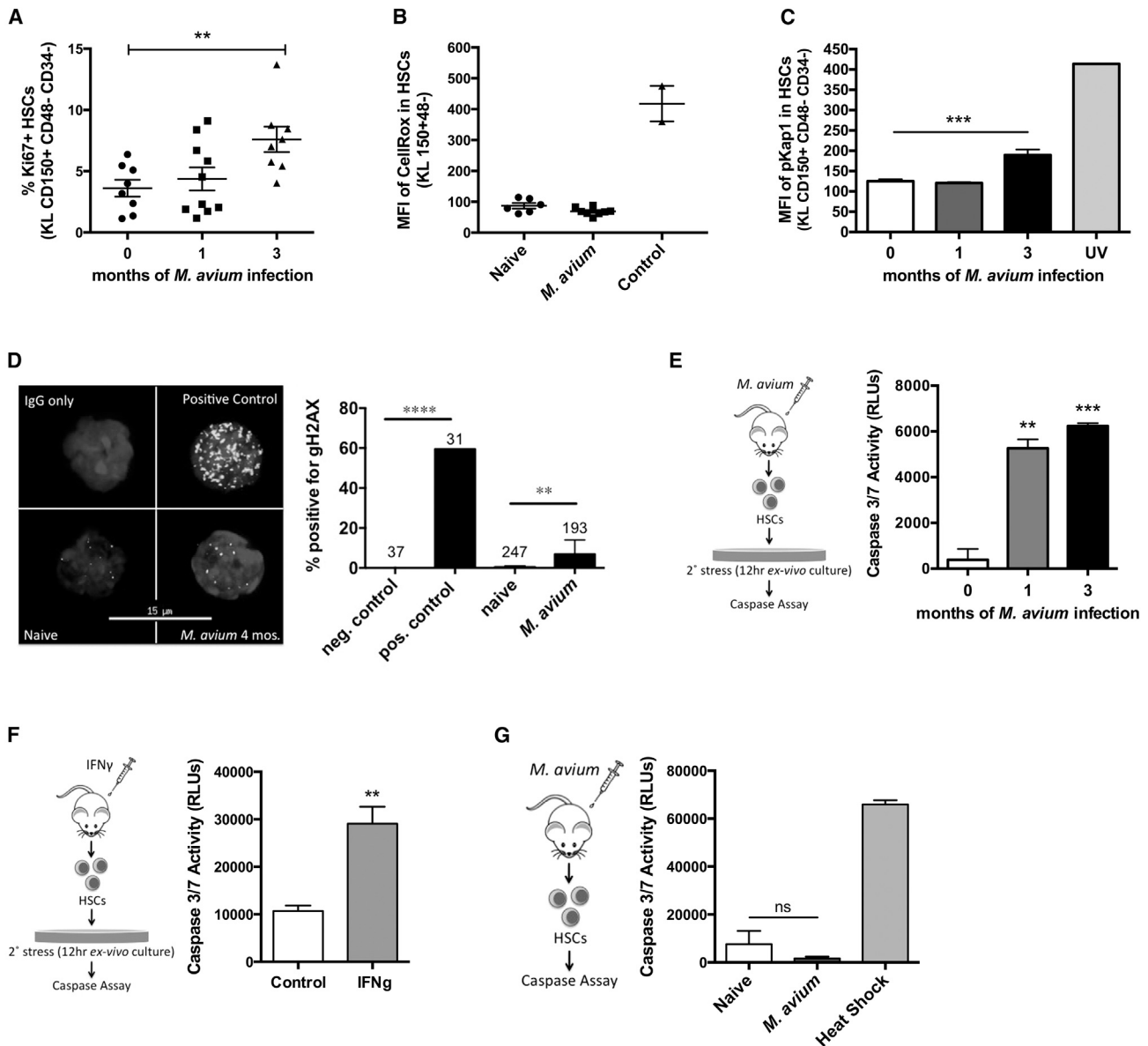


**Figure 5. HSCs from Chronically Infected Animals Have Increased Stress but No Increase in Rate of Apoptosis**

(A) Ki67<sup>+</sup> HSCs shown as percentage of total HSCs (LK CD150<sup>+</sup> CD48<sup>-</sup> CD34<sup>+</sup>) in naive, 1-month, or 3-month *M. avium*-infected mice. Data represent two independent experiments, with n = 6–10 per group.

(B) ROS levels in HSCs of naive and 4-week *M. avium*-infected mice shown as a mean fluorescent intensity (MFI) of CellRox staining. Tert-Butyl hydroperoxide (TBHP) was the positive control. Data represent two independent experiments, n = 6–8 per group.

(C) DNA damage was assessed using phospho-Kap1 (pKap1) staining of HSCs from naive or *M. avium*-infected mice. UV-treated cells were used as positive control. Data are representative of two independent studies, n = 3–5 per group.

(D) Percentage of HSCs with  $\gamma$ H2AX staining. Numbers above the bars refer to n for each condition. 1-Gy irradiation was used as a positive control. Data are representative of two independent experiments.

(E and F) Caspase 3/7 activity in 400 HSCs after 12 hr of in vitro culture. (E) HSCs from 1- or 3-month-infected mice. (F) HSCs from control or 24-hr IFN- $\gamma$ -treated mice.

(G) Caspase 3/7 activity immediately after isolation of 400 HSCs from naive or *M. avium*-infected mice.

Results for (E)–(G) are representative of two to five independent experiments, n = 3 per group. Data are presented as mean  $\pm$  SEM; \*p < 0.05, \*\*p < 0.01, \*\*\*p < 0.001, n.s., not significant. See also Figure S5.

in *lfngr1*<sup>-/-</sup> mice, suggesting that IFN- $\gamma$  signaling is required for its upregulation. In order to test the relevance of this gene in the human system, we measured *BATF2* expression in primary hu-

man CD34<sup>+</sup> cells. We found that *BATF2* expression was detectable in human CD34<sup>+</sup> progenitors and was significantly increased upon addition of IFN- $\gamma$  to the culture media (Figure 7B).

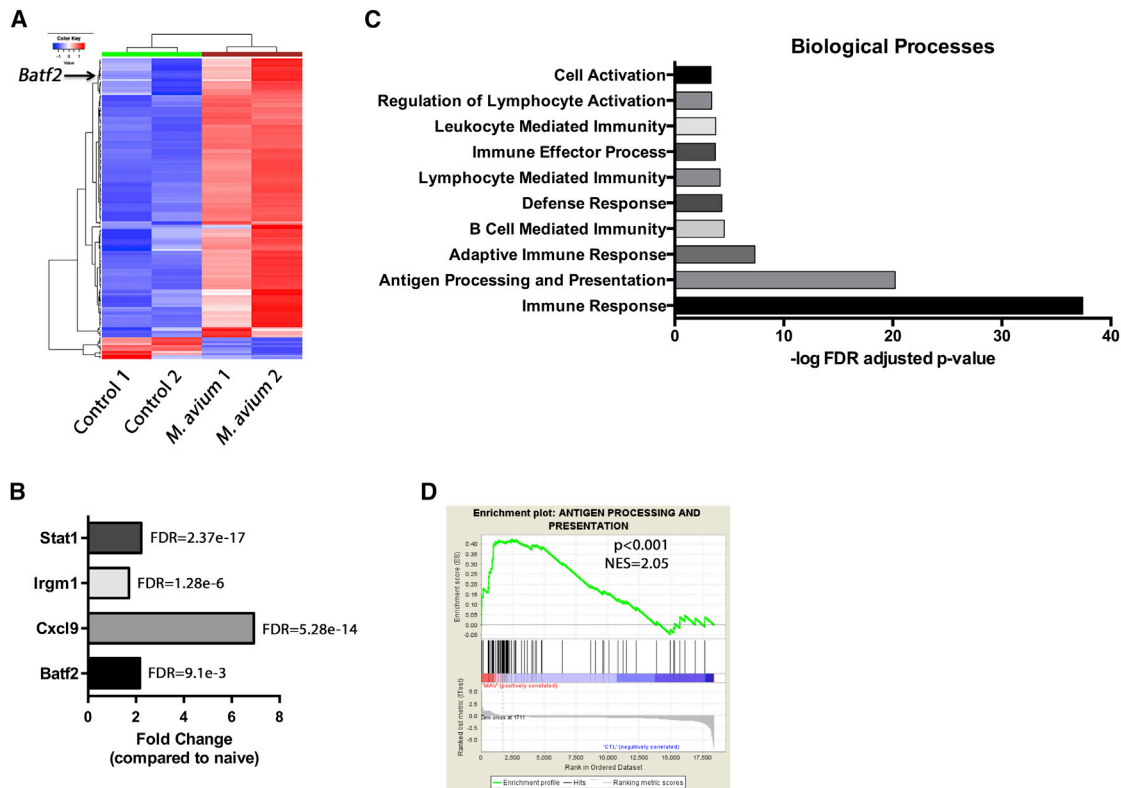


**Figure 6. Transcriptional Profiling of HSCs from Chronically Infected Animals Reveals Increased Differentiation**

(A) Heatmap of differentially expressed genes (FDR < 0.1) from RNA-seq data of naive compared to *M. avium*-infected HSCs. (B) Fold change in the normalized read counts of *Stat1*, *Irgm1*, *Cxcl9*, and *Batf2* between *M. avium*-infected and naive HSCs. (C) Gene ontology (GO) analysis of RNA-seq data from HSCs isolated from naive and 4-week *M. avium*-infected mice. Analyses were performed for differentially expressed genes with an FDR < 0.1. Log<sub>10</sub> FDR adjusted p values are shown on the x axis. (D) Gene set enrichment analysis (GSEA) was performed on RNA-seq data from naive and 4-week *M. avium*-infected mice. Antigen processing and presentation pathways are highly enriched ( $p < 0.001$ , normalized enrichment score [NES] = 2.05) in the *M. avium*-induced upregulated genes.

To test the role of *Batf2* in hematopoietic progenitors, we overexpressed *Batf2* using a retroviral vector in Sca1<sup>+</sup> murine progenitors. Overexpression was verified by qPCR (Figure S7A). Hematopoietic progenitors overexpressing *Batf2* demonstrated a trend toward increased early myeloid differentiation 8 weeks after transplantation into lethally irradiated WT recipients (Figure 7C). Since *Batf* family members are known to act in cooperation with cofactors such as *Irf1* (Roy et al., 2015), the observation that myeloid differentiation was even modestly increased without additional expression of cofactors was striking. In contrast to control cells overexpressing GFP alone, the overall engraftment of *Batf2*-overexpressing clones declined between 4 and 8 weeks post-transplant, showing that engraftment capacity is impaired (Figures 7D and 7E). These findings suggest that *Batf2*-dependent myeloid differentiation may be a mechanism for HSPC loss during chronic infection.

#### **BATF2 Loss of Function Impairs Myeloid Differentiation of Human HSPCs**

To test whether *Batf2* is required for myeloid differentiation of HSPCs, we used CRISPR-Cas9 gene editing to knock out *BATF2* in human CD34<sup>+</sup> cord-blood-derived progenitors (Gun-

dry et al., 2016; Ran et al., 2013). Four separate single-guide RNAs were designed to target the first exon of *BATF2*; spacing between PAM sequences of these guides was out of frame with one another. Genotyping by PCR revealed that the efficiency of deletion was high, with ~50% of template DNA showing a large 139-bp deletion, representing just one of the 16 potential combinations by which the four guides could disrupt the gene (Figures 7F and S7B). Gene expression was no longer detectable by real-time qPCR in the gene-edited cells, indicating a high efficiency of deletion (Figure 7G). We next conducted a differentiation assay of CD34<sup>+</sup> progenitors in vitro. Briefly, gene edited CD34<sup>+</sup> cells were incubated in complete media in the presence or absence of IFN- $\gamma$  for 3 days, and the number of HSCs (CD34<sup>+</sup>CD38<sup>-</sup>), progenitors (CD34<sup>+</sup>CD38<sup>+</sup>), and differentiated myeloid cells (CD15<sup>+</sup> or CD66b<sup>+</sup>) were counted. The final cell counts per well were not statistically different between IFN- $\gamma$ -treated and untreated groups. While HSCs were diminished in both Cas9-only control and KO cells (Figure S7C), *BATF2* KO CD34<sup>+</sup> cells differentiated less efficiently into myeloid progeny. Specifically, the IFN- $\gamma$ -mediated induction of CD66b<sup>+</sup> granulocytes was completely abrogated in KO cells (Figure 7H), while the percentage of CD15<sup>+</sup> myelomonocytic cells decreased and

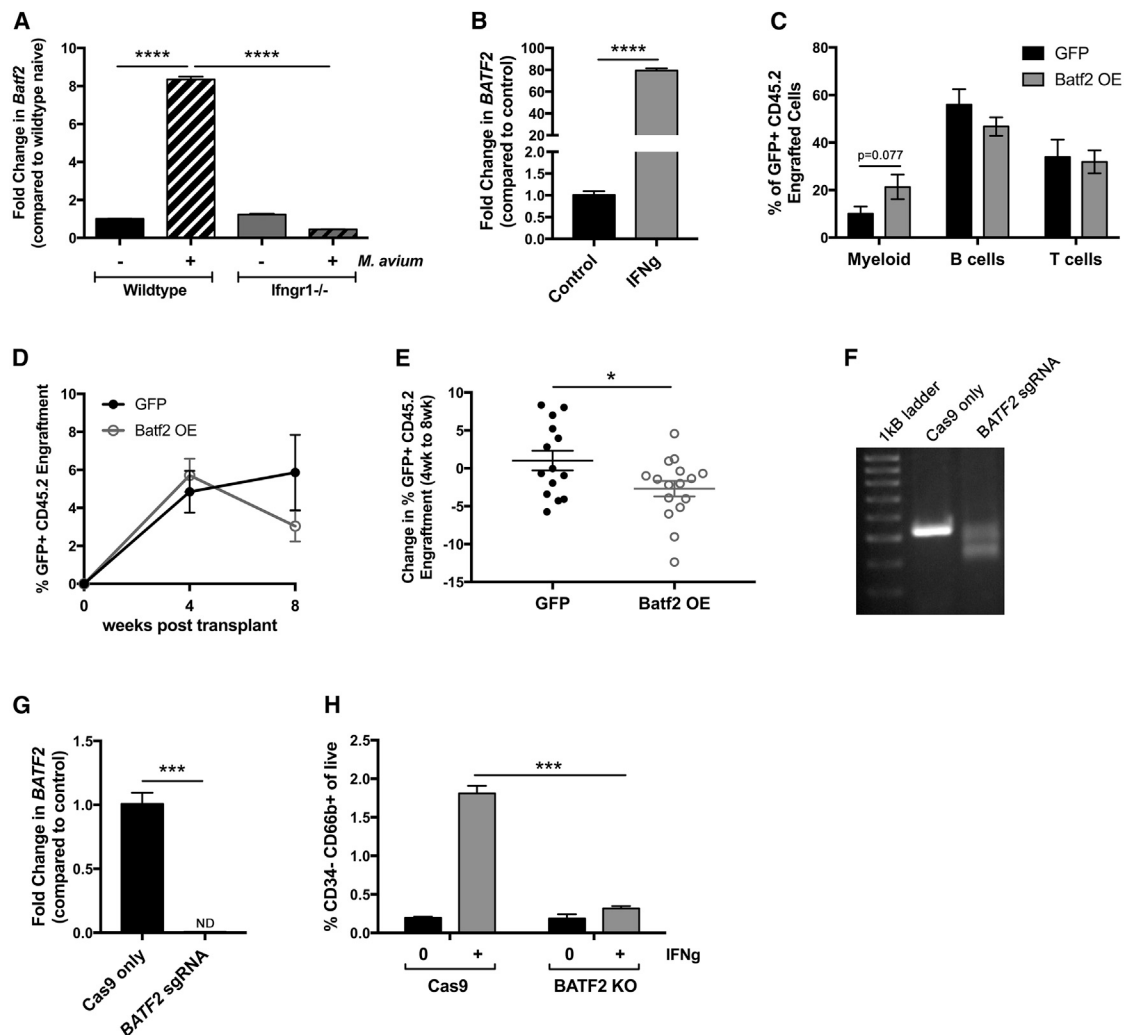


**Figure 7. Batf2 Promotes IFN- $\gamma$ -Dependent Myeloid Differentiation in Murine and Human Cells**

(A) *Batf2* RNA expression in HSCs (KL CD150<sup>+</sup> CD48<sup>-</sup> CD34<sup>-</sup>) of WT or *Ifngr1*<sup>-/-</sup> mice 4 weeks after *M. avium* infection shown as fold change over WT naive. Data are representative of two independent experiments both performed in triplicate.

(B) *BATF2* expression measured from umbilical cord-blood-derived human CD34<sup>+</sup> cells in the presence or absence of rhIFN- $\gamma$  for 3 days. Data are representative of two independent experiments using different cord blood samples, performed in triplicate.

(C–E) Sca1-enriched cells were transduced with retroviruses overexpressing GFP alone or GFP-Batf2. 2,000 CD45.2 Sca1<sup>+</sup> transduced cells were transplanted with  $2 \times 10^5$  CD45.1 rescue WBM cells. Data represent five independent experiments with  $n = 13$ –14 per group. (C) Lineage distribution of murine PB 8 weeks after transplant. (D) Engraftment of GFP<sup>+</sup> CD45.2 cells at 4 and 8 weeks post-transplant. (E) Change in engraftment of GFP<sup>+</sup> CD45.2<sup>+</sup> cells between 4 and 8 weeks post-transplant.

(F–H) Human cord-blood-derived CD34<sup>+</sup> cells after gene editing with Cas9-only control or Cas9 plus four *BATF2* single guide RNAs (sgRNAs).

(F) Representative DNA gel of *BATF2* exon 1 region.

(G) *BATF2* RNA expression. Data are representative of two independent experiments performed in triplicate.

(H) Percentage of cells that express the granulocyte marker CD66b<sup>+</sup> in the absence or presence of rhIFN- $\gamma$   $\times$  3 days. Data are representative of three independent experiments each in triplicate. Data are presented as mean  $\pm$  SEM; \* $p < 0.05$ , \*\* $p < 0.01$ , \*\*\* $p < 0.001$ , \*\*\*\* $p < 0.0001$ . See also Figure S7 and Table S3.

their absolute number trended down (Figures S7C and S7D). Meanwhile the number of CD34<sup>+</sup>CD38<sup>+</sup> progenitors in *BATF2* KO samples increased, consistent with a differentiation block (Figures S7C and S7D). These studies identify *BATF2* as a mediator of IFN- $\gamma$ -dependent terminal differentiation of human hematopoietic progenitors.

## DISCUSSION

Here, we demonstrated that chronic infection with *M. avium* leads to pancytopenia, depletion of bone marrow HSCs, and impaired HSC self-renewal. While HSCs from infected animals are exposed to increased replication stress and are more prone

to apoptosis upon secondary stress, we found no evidence of increased HSC apoptosis during *in vivo* infection. Furthermore, there was no evidence of HSC mobilization out of the bone marrow during infection. Instead, RNA profiling data pointed toward differentiation as the most significant transcriptional change. We identified *Batf2* as a potential mediator of HSPC differentiation and used gain- and loss-of-function studies to show that *Batf2* impairs HSPC persistence and is required for normal IFN- $\gamma$ -dependent myeloid differentiation in human progenitors. These studies suggest that increased terminal differentiation is the major route of HSC loss during chronic infection and provide a direct mechanism by which chronic infection causes HSC depletion.

Bone marrow suppression and pancytopenia are known complications of chronic infectious diseases including mycobacterial infections (Achi et al., 2013). Since mycobacterial infections frequently co-occur with myelofibrosis, many have assumed that pancytopenia is due to physical disruption of the bone marrow (Viallard et al., 2002). However, our data indicate that inflammatory stimulation of HSCs is a more significant contributor to pancytopenia than myelofibrosis. In another study, recruitment of bone marrow macrophages by IFN- $\gamma$  was also found to contribute to HSC dysfunction and loss (McCabe et al., 2015).

Our findings are consistent with several studies using murine knockout models to demonstrate that dysregulated IFN-signaling depletes hematopoietic progenitors, including stem cells (Essers et al., 2009; King et al., 2011; Lin et al., 2014; Sato et al., 2009). These studies using genetically modified mice suggest that artificially elevated IFN- signaling can damage self-renewal processes and deplete hematopoietic progenitor populations over time. Our study demonstrates that this occurs in the context of physiologic infection in WT mice.

Although IFN- $\gamma$  did not promote HSC mobilization, our results do not rule out the possibility that HSCs are displaced from cellular niches with the bone marrow architecture as has been shown for IFN- $\alpha$  (Kunisaki et al., 2013), nor do they rule out the possibility that HSCs in extramedullary sites could expand through self-renewal events. Prior studies have demonstrated increased apoptosis of HSPCs in aplastic anemia patients with high IFN- $\gamma$  levels through both *in vitro* and *in vivo* assays in human cells (Zeng et al., 2006). Our studies suggest that inflammation and IFN- $\gamma$  stimulation may affect HSPCs on a continuum; while we did not detect increased apoptosis during infection, we did find that the threshold for apoptosis was lowered. People with aplastic anemia may have multiple stressors, for example microenvironmental changes in the bone marrow niche in addition to increased IFN- $\gamma$  levels, that together lead to apoptosis.

We identified *Batf2* as a potential mediator of IFN- $\gamma$ -dependent terminal HSPC differentiation. Our demonstration that *BATF2* has a key role in IFN- $\gamma$ -dependent myeloid differentiation may contribute to the development of future applications to protect stem cells in the context of persistent inflammation. However, *Batf2* is likely not the only mediator of IFN- $\gamma$ -dependent myeloid differentiation, and our RNA-seq data may reveal other key regulators. In addition, although we focused on IFN- $\gamma$  as a powerful mediator of HSC loss during infection, it is almost certainly not the only one. HSCs lacking IFN- $\gamma$  receptors can

also respond to this signal indirectly via the release of interleukin-6 (IL-6) from the microenvironment (Schürch et al., 2014). Chronic LPS exposure was shown to injure HSC function (Esplin et al., 2011). A recent study reported that IL-1 proinflammatory signaling accelerates myeloid differentiation of HSPCs through activation of the transcription factor Pu.1 (Pietras et al., 2016). Other infections with less IFN- $\gamma$ -dominant inflammatory signatures may cause distinct hematological effects.

Our demonstration that HSCs are significantly depleted during chronic infection may have significant implications in the field of hematologic malignancies. Infections are epidemiologically linked to acute myelogenous leukemia (Kristinsson et al., 2011), and dysregulation of inflammation is an important contributor to aplastic anemia, which can evolve to cancer (Gañán-Gómez et al., 2015; Young and Maciejewski, 1997). Given recent reports of clonal hematopoiesis as a risk factor for malignancy (Yoshizato et al., 2015), attrition in HSC numbers due to persistent inflammation could provide a pathophysiologic basis for these links. Further work to delineate the effects of inflammation on HSCs is likely to yield important mechanistic insight into other diseases of HSC malfunction, including transient bone marrow suppression, aplastic anemia, myelodysplastic syndrome, and leukemia.

## EXPERIMENTAL PROCEDURES

### Mice

Wild-type C57BL/6 (CD45.2) and C57BL/6.SJL (CD45.1) mice 6–12 weeks of age were used. C57BL/6 *Ifngr1<sup>-/-</sup>* (Stock #3288) mice were obtained from Jackson Laboratory. All mice were maintained at an AALAC-accredited, specific pathogen-free animal facility at Baylor College of Medicine. All experiments were approved by the institutional review board of Baylor College of Medicine. Genotypes were confirmed by PCR.

### Microbial Infections

Mice were infected monthly with  $2 \times 10^8$  colony-forming units of *Mycobacterium avium* i.v. as described (Feng et al., 2008). *M. avium* was detected by growth on Middlebrook agar and by PCR (Park et al., 2000).

### Bone Marrow Transplantation

Non-competitive bone marrow transplants were performed by intravenous (i.v.) injection of CD45.2 donor WBM cells from infected mice or naive controls into lethally irradiated CD45.1 WT recipients. For competitive transplants, CD45.2 donor WBM cells from naive or infected mice were mixed with wild-type CD45.1 competitor WBM cells prior to injection into CD45.1 recipients. For secondary transplants, sorted CD45.2 donor HSCs were isolated from primary recipients and transplanted with CD45.1 rescue WBM into naive CD45.1 irradiated recipients.

### RNA Purification and RNA-Seq

Approximately 70,000 HSCs (SP<sup>L<sup>SK</sup></sup>CD150<sup>+</sup>) were sorted into Trizol from the pools of naive or infected mice. RNA was isolated with the RNeasy Micro column (QIAGEN). Illumina HiSeq was used for sequencing with a paired-end sequencing length of 100 bp. False discovery rate (FDR) <0.05 was considered statistically significant. Gene ontology and pathway analyses were performed for differentially expressed genes with FDR <0.1.

### Flow Cytometry

PB was analyzed with a Hemavet 950. SP staining was performed with Hoechst 33342 (Sigma) as previously described (Goodell et al., 1996). Myeloid-biased and lymphoid-biased HSCs were identified as previously described (Challen et al., 2010). A full list of all staining schemes and antibodies is provided in Tables S4 and S5.

### Colony-Forming Assays

Colony-forming assays were performed by plating WBM cells in methylcellulose media and counting colonies after 9 days (STEMCELL Technologies).

### Single-Cell Assays

Single HSCs (KSL CD150<sup>+</sup> CD48<sup>-</sup> CD34<sup>-</sup>) were sorted into 96-well plates containing StemSpan media, and colonies were counted after 10 days.

### Cell Proliferation and DNA Damage

Proliferation and DNA damage of HSCs was determined using flow cytometry of cells co-stained with Ki67 and pKap1.  $\gamma$ H2AX staining was performed on sorted HSCs from naive or 4-month *M. avium*-infected mice as previously described (Walter et al., 2015).

### Reactive Oxygen Species

Levels of ROS within HSCs from control or infected mice were determined by flow cytometry analysis of cells stained with Molecular Probes' CellRox Green Flow Cytometry Assay Kit (Life Technologies) according to the manufacturer's protocol.

### Apoptosis Assays

Apoptosis was determined using the Caspase-Glo 3/7 Assay (Promega). HSCs were sorted directly into 96-well plates containing StemSpan media and Caspase Glo reagent was either immediately added to the wells or was added after 12 hr incubation at 37°C.

### Batf2 Overexpression and BATF2 Deletion

Batf2 was overexpressed in Sca1<sup>+</sup> cells using a retrovirus as previously described (Ergen et al., 2012). Sca1<sup>+</sup> CD45.2 cells were transplanted into lethally irradiated CD45.1 recipient mice along with rescue marrow, and engraftment of the GFP<sup>+</sup> CD45.2 cells was tracked every 4 weeks. BATF2 deletion was conducted as described (Gundry et al., 2016). For each experiment, CD34<sup>+</sup> cells were isolated from an unrelated frozen human umbilical cord blood or Buffy coat sample. Four single-guide RNAs (Table S3) were mixed with recombinant Cas9 protein and transduced into CD34<sup>+</sup> cells by electroporation. Gene deletion was confirmed by PCR and qPCR. Differentiation of human cells was measured by incubation of CD34<sup>+</sup> cells with IFN- $\gamma$  for 3 days. HSPCs and differentiated myeloid cells were characterized by flow cytometry.

### Mobilization Assays

Mice were treated with G-CSF for 6 days and/or rmlFN- $\gamma$  for 24 hr prior to sacrifice. HSCs were detected in the spleen by flow cytometry. For transplants, splenocytes were mixed with CD45.1 rescue WBM cells and transplanted into lethally irradiated CD45.1 recipients.

### Estimation of HSC Loss

The basis for understanding the dynamics of HSC loss is the differential equation of the form  $\dot{N}(t) = -\lambda N(t) + 2(1-d)\lambda N(t)$  where  $N(t)$  is the HSC count at time  $t$ ,  $\lambda$  is the division rate of the HSC, and  $d$  is the fraction of HSC progeny that are not HSC (i.e., that constitutes HSC "loss"). The equation admits explicit solution  $N(t) = N(0)\exp[(1-2d)\lambda t]$ , where the initial condition  $N(0)$  is equal to the pre-infection steady-state HSC count. Logarithm of the HSC count is a linear function of  $\ln[N(0)]$  and  $d$ , and therefore these two quantities can be estimated using standard linear regression, if the value of  $\lambda$  is assumed (we set  $\lambda = 0.05 \text{ d}^{-1}$ ) (Wilson et al., 2008). Given that (1) each measurement corresponds to a different mouse (represented by the asterisks in Figure S1G), and (2) HSC counts show wide interindividual variability, we estimated the variability in any time point with at least two replicates by fitting a gamma distribution. Then we fit regression lines to the quantiles of orders 2.5%, 5%, 25%, 50%, 75%, 95%, and 97.5% of the gamma distributions. These lines (Figure S1G) provide corresponding quantile values of  $N(0)$  and  $d$  (Table S1), yielding the 95% confidence interval for  $d$ .

### Statistics

Mean values  $\pm$  SEM are shown. Student's *t* test or two-way ANOVA were used for comparisons (GraphPad Prism v.5.0).

See Supplemental Experimental Procedures for more details.

### ACCESSION NUMBERS

The accession number for the RNA-seq data reported in this paper is GEO: GSE89364.

### SUPPLEMENTAL INFORMATION

Supplemental Information includes Supplemental Experimental Procedures, seven figures, and five tables and can be found with this article online at <http://dx.doi.org/10.1016/j.celrep.2016.11.031>.

### AUTHOR CONTRIBUTIONS

Conceptualization, K.Y.K.; Investigation, K.A.M., M.J., and K.Y.K.; Formal Analysis, S.C., F.C., D.S., Q.M., and M.K.; Writing, K.A.M. and K.Y.K.; Supervision, K.Y.K.

### ACKNOWLEDGMENTS

We thank C. Kadmon, A. Rosen, and Y. Zheng for technical assistance; M. Goodell and D. Nakada for useful discussions regarding this work; C. Gillespie for reviewing the manuscript; and the Texas Advanced Computing Center (TACC) at The University of Texas at Austin for providing HPC resources for the data analysis. This project was supported by the Cytometry and Cell Sorting Core (NIAID P30AI036211, NCI P30CA125123, NCI P30CA125123, NCI P30CA125123, NCI P30CA125123, NCI P30CA125123) and the Integrated Microscopy Core (HD007495, DK56338, CA125123) at Baylor College of Medicine with additional funding from the Dan L. Duncan Cancer Center and the John S. Dunn Gulf Coast Consortium for Chemical Genetics. This work was supported by grants from the NIDDK DK060445 (K.A.M.), the NHLBI HL128173-02 (M.K. and S.C.) and K08HL098898 (K.Y.K.), and the Department of Defense IDEA award in bone marrow failure research (10505346), the Caroline Wiess Law Foundation for Molecular Medicine, the Aplastic Anemia and MDS International Foundation Liviya Anderson Award, and a March of Dimes Basil O'Connor Starter Scholar Award (K.Y.K.).

Received: December 24, 2015

Revised: October 2, 2016

Accepted: November 9, 2016

Published: December 6, 2016

### REFERENCES

- Achi, H.V., Ahui, B.J., Anon, J.C., Kouassi, B.A., Dje-Bi, H., and Kininman, H. (2013). [Pancytopenia: A severe complication of miliary tuberculosis]. *Rev. Mal. Respir.* 30, 33–37.
- Baldrige, M.T., King, K.Y., Boles, N.C., Weksberg, D.C., and Goodell, M.A. (2010). Quiescent haematopoietic stem cells are activated by IFN- $\gamma$  in response to chronic infection. *Nature* 465, 793–797.
- Baldrige, M.T., King, K.Y., and Goodell, M.A. (2011). Inflammatory signals regulate hematopoietic stem cells. *Trends Immunol.* 32, 57–65.
- Balmer, M.L., Schürch, C.M., Saito, Y., Geuking, M.B., Li, H., Cuenca, M., Kovtonyuk, L.V., McCoy, K.D., Hapfelmeier, S., Ochsenbein, A.F., et al. (2014). Microbiota-derived compounds drive steady-state granulopoiesis via MyD88/TICAM signaling. *J. Immunol.* 193, 5273–5283.
- Challen, G.A., Boles, N.C., Chambers, S.M., and Goodell, M.A. (2010). Distinct hematopoietic stem cell subtypes are differentially regulated by TGF- $\beta$ 1. *Cell Stem Cell* 6, 265–278.
- Ergen, A.V., Boles, N.C., and Goodell, M.A. (2012). Rantes/Ccl5 influences hematopoietic stem cell subtypes and causes myeloid skewing. *Blood* 119, 2500–2509.
- Esplin, B.L., Shimazu, T., Welner, R.S., Garrett, K.P., Nie, L., Zhang, Q., Humphrey, M.B., Yang, Q., Borghesi, L.A., and Kincade, P.W. (2011). Chronic exposure to a TLR ligand injures hematopoietic stem cells. *J. Immunol.* 186, 5367–5375.

- Essers, M.A.G., Offner, S., Blanco-Bose, W.E., Waibler, Z., Kalinke, U., Duchosal, M.A., and Trumpp, A. (2009). IFN $\alpha$  activates dormant haematopoietic stem cells in vivo. *Nature* 458, 904–908.
- Feng, C.G., Weksberg, D.C., Taylor, G.A., Sher, A., and Goodell, M.A. (2008). The p47 GTPase Lrg-47 (*Irgm1*) links host defense and hematopoietic stem cell proliferation. *Cell Stem Cell* 2, 83–89.
- Fitzgerald, D., and Haas, D.W. (2005). *Mycobacterium tuberculosis*. In *Principles and Practice of Infectious Diseases*, G.L. Mandell, J.E. Bennett, and R. Dolin, eds. (Elsevier), pp. 2852–2886.
- Flórido, M., Pearl, J.E., Solache, A., Borges, M., Haynes, L., Cooper, A.M., and Appelberg, R. (2005). Gamma interferon-induced T-cell loss in virulent *Mycobacterium avium* infection. *Infect. Immun.* 73, 3577–3586.
- Gañán-Gómez, I., Wei, Y., Starczynowski, D.T., Colla, S., Yang, H., Cabrero-Calvo, M., Bohannan, Z.S., Verma, A., Steidl, U., and Garcia-Manero, G. (2015). Deregulation of innate immune and inflammatory signaling in myelodysplastic syndromes. *Leukemia* 29, 1458–1469.
- Goodell, M.A., Brose, K., Paradis, G., Conner, A.S., and Mulligan, R.C. (1996). Isolation and functional properties of murine hematopoietic stem cells that are replicating in vivo. *J. Exp. Med.* 183, 1797–1806.
- Gundry, M.C., Brunetti, L., Lin, A., Mayle, A.E., Kitano, A., Wagner, D., Hsu, J.I., Hoegenauer, K.A., Rooney, C.M., Goodell, M.A., and Nakada, D. (2016). Highly efficient genome editing of murine and human hematopoietic progenitor cells by CRISPR/Cas9. *Cell Rep.* 17, 1453–1461.
- King, K.Y., Baldrige, M.T., Weksberg, D.C., Chambers, S.M., Lukov, G.L., Wu, S., Boles, N.C., Jung, S.Y., Qin, J., Liu, D., et al. (2011). *Irgm1* protects hematopoietic stem cells by negative regulation of IFN signaling. *Blood* 118, 1525–1533.
- King, K.Y., and Goodell, M.A. (2011). Inflammatory modulation of HSCs: Viewing the HSC as a foundation for the immune response. *Nat. Rev. Immunol.* 11, 685–692.
- Kristinsson, S.Y., Björkholm, M., Hultcrantz, M., Derolf, Å.R., Landgren, O., and Goldin, L.R. (2011). Chronic immune stimulation might act as a trigger for the development of acute myeloid leukemia or myelodysplastic syndromes. *J. Clin. Oncol.* 29, 2897–2903.
- Kunisaki, Y., Bruns, I., Scheiermann, C., Ahmed, J., Pinho, S., Zhang, D., Mizoguchi, T., Wei, Q., Lucas, D., Ito, K., et al. (2013). Arteriolar niches maintain haematopoietic stem cell quiescence. *Nature* 502, 637–643.
- Lin, F.C., Karwan, M., Saleh, B., Hodge, D.L., Chan, T., Boelte, K.C., Keller, J.R., and Young, H.A. (2014). IFN- $\gamma$  causes aplastic anemia by altering hematopoietic stem/progenitor cell composition and disrupting lineage differentiation. *Blood* 124, 3699–3708.
- Matatall, K.A., Shen, C.C., Challen, G.A., and King, K.Y. (2014). Type II interferon promotes differentiation of myeloid-biased hematopoietic stem cells. *Stem Cells* 32, 3023–3030.
- McCabe, A., Zhang, Y., Thai, V., Jones, M., Jordan, M.B., and MacNamara, K.C. (2015). Macrophage-lineage cells negatively regulate the hematopoietic stem cell pool in response to interferon gamma at steady state and during infection. *Stem Cells* 33, 2294–2305.
- Nagai, Y., Garrett, K.P., Ohta, S., Bahrn, U., Kouro, T., Akira, S., Takatsu, K., and Kincaid, P.W. (2006). Toll-like receptors on hematopoietic progenitor cells stimulate innate immune system replenishment. *Immunity* 24, 801–812.
- Notta, F., Zandi, S., Takayama, N., Dobson, S., Gan, O.I., Wilson, G., Kaufmann, K.B., McLeod, J., Laurenti, E., Dunant, C.F., et al. (2016). Distinct routes of lineage development reshape the human blood hierarchy across ontogeny. *Science* 351, aab2116.
- Park, H., Jang, H., Kim, C., Chung, B., Chang, C.L., Park, S.K., and Song, S. (2000). Detection and identification of mycobacteria by amplification of the internal transcribed spacer regions with genus- and species-specific PCR primers. *J. Clin. Microbiol.* 38, 4080–4085.
- Pietras, E.M., Lakshminarasimhan, R., Techner, J.M., Fong, S., Flach, J., Binnewies, M., and Passegué, E. (2014). Re-entry into quiescence protects hematopoietic stem cells from the killing effect of chronic exposure to type I interferons. *J. Exp. Med.* 211, 245–262.
- Pietras, E.M., Mirantes-Barbeito, C., Fong, S., Loeffler, D., Kovtonyuk, L.V., Zhang, S., Lakshminarasimhan, R., Chin, C.P., Techner, J.M., Will, B., et al. (2016). Chronic interleukin-1 exposure drives haematopoietic stem cells towards precocious myeloid differentiation at the expense of self-renewal. *Nat. Cell Biol.* 18, 607–618.
- Ramos-Casals, M., García-Carrasco, M., López-Medrano, F., Trejo, O., Forns, X., López-Guillermo, A., Muñoz, C., Ingelmo, M., and Font, J. (2003). Severe autoimmune cytopenias in treatment-naive hepatitis C virus infection: Clinical description of 35 cases. *Medicine (Baltimore)* 82, 87–96.
- Ran, F.A., Hsu, P.D., Wright, J., Agarwala, V., Scott, D.A., and Zhang, F. (2013). Genome engineering using the CRISPR-Cas9 system. *Nat. Protoc.* 8, 2281–2308.
- Roy, S., Guler, R., Parihar, S.P., Schmeier, S., Kaczkowski, B., Nishimura, H., Shin, J.W., Negishi, Y., Oztürk, M., Hurdal, R., et al. (2015). *Batf2/Irf1* induces inflammatory responses in classically activated macrophages, lipopolysaccharides, and mycobacterial infection. *J. Immunol.* 194, 6035–6044.
- Santos, M.A., Faryabi, R.B., Ergen, A.V., Day, A.M., Malhowski, A., Canela, A., Onozawa, M., Lee, J.E., Callen, E., Gutierrez-Martinez, P., et al. (2014). DNA-damage-induced differentiation of leukaemic cells as an anti-cancer barrier. *Nature* 514, 107–111.
- Sato, T., Onai, N., Yoshihara, H., Arai, F., Suda, T., and Ohteki, T. (2009). Interferon regulatory factor-2 protects quiescent hematopoietic stem cells from type I interferon-dependent exhaustion. *Nat. Med.* 15, 696–700.
- Scadden, D.T., Zon, L.I., and Gropman, J.E. (1989). Pathophysiology and management of HIV-associated hematologic disorders. *Blood* 74, 1455–1463.
- Schürch, C.M., Riether, C., and Ochsenbein, A.F. (2014). Cytotoxic CD8+ T cells stimulate hematopoietic progenitors by promoting cytokine release from bone marrow mesenchymal stromal cells. *Cell Stem Cell* 14, 460–472.
- Takizawa, H., Boettcher, S., and Manz, M.G. (2012). Demand-adapted regulation of early hematopoiesis in infection and inflammation. *Blood* 119, 2991–3002.
- Tussiwand, R., Lee, W.L., Murphy, T.L., Mashayekhi, M., Kc, W., Albring, J.C., Satpathy, A.T., Rotondo, J.A., Edelson, B.T., Kretzer, N.M., et al. (2012). Compensatory dendritic cell development mediated by BATF-IRF interactions. *Nature* 490, 502–507.
- Viallard, J.F., Parrons, M., Boiron, J.M., Texier, J., Mercie, P., and Pellegrin, J.L. (2002). Reversible myelofibrosis induced by tuberculosis. *Clin. Infect. Dis.* 34, 1641–1643.
- Walter, D., Lier, A., Geiselhart, A., Thalheimer, F.B., Huntscha, S., Sobotta, M.C., Moehrl, B., Brocks, D., Bayindir, I., Kaschutnig, P., et al. (2015). Exit from dormancy provokes DNA-damage-induced attrition in haematopoietic stem cells. *Nature* 520, 549–552.
- Wang, J., Sun, Q., Morita, Y., Jiang, H., Gross, A., Lechel, A., Hildner, K., Guachalla, L.M., Gompf, A., Hartmann, D., et al. (2012). A differentiation checkpoint limits hematopoietic stem cell self-renewal in response to DNA damage. *Cell* 148, 1001–1014.
- Wilson, A., Laurenti, E., Oser, G., van der Wath, R.C., Blanco-Bose, W., Jaworski, M., Offner, S., Dunant, C.F., Eshkind, L., Bockamp, E., et al. (2008). Hematopoietic stem cells reversibly switch from dormancy to self-renewal during homeostasis and repair. *Cell* 135, 1118–1129.
- Yang, L., Dybedal, I., Bryder, D., Nilsson, L., Sitnicka, E., Sasaki, Y., and Jacobsen, S.E.W. (2005). IFN-gamma negatively modulates self-renewal of repopulating human hemopoietic stem cells. *J. Immunol.* 174, 752–757.
- Yoshizato, T., Dumitriu, B., Hosokawa, K., Makishima, H., Yoshida, K., Townsley, D., Sato-Otsubo, A., Sato, Y., Liu, D., Suzuki, H., et al. (2015). Somatic mutations and clonal hematopoiesis in aplastic anemia. *N. Engl. J. Med.* 373, 35–47.
- Young, N.S., and Maciejewski, J. (1997). The pathophysiology of acquired aplastic anemia. *N Engl J Med.* 336, 1365–1372.
- Zeng, W., Miyazato, A., Chen, G., Kajigaya, S., Young, N.S., and Maciejewski, J.P. (2006). Interferon-gamma-induced gene expression in CD34 cells: Identification of pathologic cytokine-specific signature profiles. *Blood* 107, 167–175.